Meteoritics & Planetary Science 38, Nr 4, 565–578 (2003)
Abstract available online at http://meteoritics.org

Magnetic fields of lunar multi-ring impact basins

J. S. HALEKAS,* R. P. LIN, and D. L. MITCHELL

Space Sciences Laboratory, University of California, Berkeley, California 94720, USA
*Corresponding author. E-mail: jazzman@ssl.berkeley.edu

(Received 15 October 2002; revision accepted 26 March 2003)

Abstract–We survey the magnetic fields of lunar multi-ring impact basins using data from the electron reflectometer instrument on the Lunar Prospector spacecraft. As for smaller lunar craters, the primary signature is a magnetic low that extends to ~1.5–2 basin radii, suggesting shock demagnetization of relatively soft crustal magnetization. A secondary signature, as for large terrestrial basins, is the presence of central magnetic anomalies, which may be due to thermal remanence in impact melt rocks and/or shock remanence in the central uplift. The radial extent of the anomalies may argue for the former possibility, but the latter or a combination of the two are also possible. Central anomaly fields are absent for the oldest pre-Nectarian basins, increase to a peak in early Nectarian basins, and decrease to a low level for Imbrian basins. If basin-associated anomalies provide a good indication of ambient magnetic fields when the basins formed, this suggests the existence of a "magnetic era" (possibly due to a lunar core dynamo) similar to that implied by paleointensity results from returned lunar samples. However, the central basin anomalies suggest that the fields peaked in early Nectarian times and were low in Imbrian times, while samples provide evidence for high fields in Nectarian and early Imbrian times.

INTRODUCTION

Large multi-ring impact basins, many of which have been subsequently covered by mare basalt flows, are the most prominent geological features on the moon. Impact basins are created by hypervelocity impacts, which release tremendous amounts of energy (for a detailed discussion of the basin-forming process, see Melosh (1989) or Spudis (1993)). This energy is manifested in the form of shock waves with peak pressures of hundreds of GPa radiating from the impact point, which in turn cause significant heating, especially near the impact point. Both shock and heating have significant effects upon the magnetization of minerals. In the absence of a strong ambient magnetic field, both shock and thermal effects tend to demagnetize magnetic carriers, while in the presence of a strong field, both can produce stable remanent magnetization. Therefore, one expects that lunar impact basins should have significant magnetic signatures. This is certainly the case on Earth, where magnetic anomalies have become an important tool in the recognition and study of impact structures (Pilkington and Grieve 1992). Now, with new data from the electron reflectometer instrument on Lunar Prospector (LP), we have identified a number of basin-associated magnetic features on the moon.

The first measurements of lunar crustal magnetic fields were made by experiments on the Apollo subsatellites (Coleman et al. 1972; Anderson et al. 1976). Apollo data showed (Lin et al. 1988), and LP data confirmed (Hood et al. 2001), that the largest regions of strong magnetic fields (some more than a thousand km across, with fields of tens to hundreds of nT) lie on the lunar far side, diametrically opposite (antipodal) to the young large Orientale, Imbrium, Serenitatis, Crisium, and (to a lesser extent) Nectaris impact basins. Shock remanence generated by a combination of magnetic field amplification by plasma compression and focussing of seismic waves and/or solid ejecta may be responsible for these antipodal signatures (Hood and Huang 1991). Meanwhile, LP observations show that, in contrast to the antipodal regions, impact craters and basins of Imbrian age and younger tend to have weak magnetic fields (0–1.5 nT) (Halekas et al. 2001, 2002a), suggesting impact demagnetization.

The magnetic signatures of lunar craters with diameters from 50 km to a few hundred km were investigated in detail using LP electron reflectometer data (Halekas et al. 2002a). Careful corrections for the effects of surface electrostatic charging (Halekas et al. 2002b) allowed more sensitive measurements of the weakest lunar magnetic fields than ever

before. This recent study found that craters of all ages have associated magnetic lows. Demagnetization signatures extend to ~2–4 crater radii, suggesting shock rather than thermal demagnetization. Younger craters are more likely to have clear and complete demagnetization signatures, suggesting that many older crater-associated magnetic lows have been subsequently obscured. The lack of significant crater-associated edge effects (which should be seen in the case of demagnetization of part of a region of uniform magnetization) or a clear dependence on crater size (which should be seen if demagnetization for all craters surveyed did not extend below the base of the magnetized layer) were used to constrain the depth and coherence scale of lunar crustal magnetization to <25–50 km. If lunar crustal magnetization had a coherence scale this small when originally emplaced, it suggests its production by some transient process. However, the cumulative effects of subsequent impacts could also have reduced the coherence of magnetization that was originally more uniform.

We now investigate the magnetic fields of lunar multi-ring impact basins. We include basins with two or more currently observable rings (including peak-ring basins), and those which are large enough that they likely had multiple rings (though so degraded that they are no longer observable). The primary magnetic signature for many lunar basins is a wide magnetic low, just as for smaller craters. However, the most recent high resolution LP data has allowed us to identify other shorter wavelength magnetic features associated with lunar basins. We find that older basins are especially likely to have such central magnetic anomalies. This study will attempt to characterize the magnetic field signatures observed for lunar impact basins of all ages.

We can gain some appreciation for the magnetic fields that may be expected for lunar basins by studying the fields observed for terrestrial basins. On the Earth, a wide variety of different magnetic signatures are observed over impact craters and basins. For smaller terrestrial craters (diameters <10 km), a smooth and simple magnetic low is usually observed (Pilkington and Grieve 1992). Reduced magnetic fields are also sometimes seen in larger structures, but the magnetic low is often modified by the presence of magnetic anomalies of large amplitude but short wavelength at or near the crater center. Study of terrestrial impact basins has revealed that all terrestrial basins with diameters greater than 40 km, and some smaller than this, have magnetic anomalies in the center of the basins, primarily due to remanent rather than induced magnetization (Pilkington and Grieve 1992). These range from short-wavelength anomalies with a radial extent of a fraction of the transient cavity radius (e.g., those in the Haughton, Manicougan, and Lake St. Martin basins (Pohl et al. 1988; Coles and Clark 1978, 1982)), to larger groups of anomalies that fill most of the transient cavity (e.g. the outer ring of magnetic anomalies in the Chicxulub basin (Pilkington and Hildebrand 1994) or the central anomaly in the Bosumtwi crater (Plado et al. 2000)). The more localized anomalies have generally been ascribed to shock remanent magnetization (SRM) or chemical remanent magnetization (which should not be a factor in the highly reducing lunar environment) in the unmelted central uplift region, while anomalies that roughly fill the transient cavity region have generally been interpreted as thermal remanent magnetization (TRM) in melt-rich suevite breccias and/or impact melt rocks. Either interpretation requires the presence of a strong ambient magnetic field. In the case of TRM, this field must remain steady while the impact site cools below the Curie point. However, in the case of SRM, the field could be transient in nature. In the terrestrial case, most authors have assumed that the magnetizing field is the Earth's dynamo field. Where magnetization directions have been determined, they are generally consistent with this picture of remanence acquisition in the Earth's dynamo field (Coles and Clark 1978, 1982; Pilkington and Grieve 1992; Plado et al. 2000).

We do not expect lunar basins to have exactly the same kind of magnetic signatures as terrestrial basins of the same size. Though the impact process is essentially the same on different planets, the growth of impact craters and basins is controlled by gravity, and data from Mars, Earth, and the moon suggests that impact structures scale morphologically as ~1/g (Pike 1980). Therefore, a terrestrial basin with a diameter of 40 km is roughly morphologically equivalent to a lunar basin with a diameter of 240 km. Also, on Earth, impact basins formed in the presence of a strong magnetic field, while on the moon this may or may not have been the case. Finally, lunar magnetic carriers and their properties vary greatly from terrestrial ones, with native iron metal the main lunar magnetic carrier (Fuller 1974) and iron oxides the main terrestrial ones. Nonetheless, we will see that the magnetic signatures observed for lunar basins resemble those of terrestrial impact basins.

MAGNETIC FIELDS OF LUNAR IMPACT BASINS: OBSERVATIONS

It has not proven possible to absolutely date most lunar impact basins (though much effort has been made to associate returned samples with specific impact events). One can, however, date impact basins relative to each other by using superposition relations and crater counting statistics. We list the 34 youngest lunar basins (as described by Wilhelms [1984]), along with their positions, main ring diameters, transient cavity diameters, relative ages (I = Imbrian (~3.2–3.85 Gyr), N = Nectarian (~3.850–3.92 Gyr), P = pre-Nectarian (>~3.92 Gyr)) and general magnetic characteristics (L = magnetic low, M = central magnetic anomaly, NS = no signature, ND = insufficient data coverage) in order of increasing age in Table 1.

Where possible, the Imbrian, Nectarian, and pre-Nectarian age groups have been further subdivided by adding a numerical index which increases from 1 for the youngest

Table 1. Post-Australe lunar impact basins.

Basin name	Deg. long.	Deg. lat.	Main ring diameter	Trans. cav. diameter	Age	Mag. sig.
Orientale	–95	–20	930	397 (WP)	I-1	L/M
Schrodinger	134	–75	320	191 (C)	I-2	L
Imbrium	–18	33	1200	744 (WP)	I-3	L/M
Sikorsky-Rittenhouse	111	–69	310	187 (C)	N-4	L
Bailly	–68	–67	300	182 (C)	N-4	M
Hertzsprung	–129	2	570	308 (C)	N-4	L
Serenitatis	19	27	740 (920)	657 (WP)	N-4	L
Crisium	59	18	635 (740)	487 (WP)	N-4	M
Humorum	–40	–24	440	358 (WP)	N-4	L/M
Humboldtianum	84	61	600	331 (WP)	N-4	L/M
Mendeleev	141	6	330	197 (C)	N-5	L/M
Mendel-Rydberg	–94	–50	630 (420)	281 (WP)	N-6	M
Korolev	–157	–5	440	249 (C)	N-6	NS
Moscoviense	147	26	445	252 (C)	N-6	M
Nectaris	34	–16	860	414 (WP)	N-6	L/M
Apollo	–151	–36	505	279 (C)	P-7	M
Grimaldi	–68	–5	430	198 (WP)	P-7	L
Freundlich-Sharonov	175	19	600	321 (C)	P-8	L/M
Birkhoff	–147	59	330	197 (C)	P-9	L/M
Planck	136	–58	325	194 (C)	P-9	M
Schiller-Zucchius	–45	–56	325	194 (C)	P-9	L/M
Amundsen-Ganswindt	120	–81	355	209 (C)	P-9	ND
Lorentz	–97	34	360	211 (C)	P-10	L/M
Smythii	87	–2	840 (740)	443 (WP)	P-11	NS
Coulomb-Sarton	–123	52	530 (440)	290 (C)	P-11	L
Keeler-Heaviside	162	–10	780 (500)	399 (C)	P-12	NS
Poincare	162	–58	340	202 (C)	P-12	L
Ingenii	163	–34	560 (315)	304 (C)	P-12	NS
Lomonosov-Fleming	105	19	620	330 (C)	P-13	NS
Nubium	–15	–21	690	360 (C)	P-13	L
Fecunditatis	52	–4	690	360 (C)	P-13	NS
Mutus-Vlacq	21	–52	700	365 (C)	P-13	ND
Tranquilitatis	40	7	775 (700)	396 (C)	P-13	L
Australe	95	–52	880	440 (C)	P-13	NS

Imbrian basin (Orientale) to 13 for the oldest pre-Nectarian basin considered (Australe). It is possible to distinguish the relative ages of basins in different subdivided age groups (e.g., Imbrium and Schrodinger, in the I-1 and I-2 age groups respectively), but not those of basins in the same group (e.g., Humorum and Humboldtianum, both in the N-4 age group). For the Humorum and Crisium basins, we have adopted a smaller main ring diameter than that originally preferred by Wilhelms (1984) (these diameters were considered uncertain in that work). Where substantially different estimates were obtained by Spudis (1993), we list them in parentheses.

It is currently believed that the final morphology of an impact basin is the result of the collapse of a smaller and deeper structure (Melosh and Ivanov 1999). The transient cavity represents the limit of material displaced outward by the basin-forming process (as opposed to the excavation cavity, which is the limit of excavated material; the transient and excavation cavities have the same diameter, but the excavation cavity is not as deep). The transient cavity is in some sense an idealization that never physically exists. However, research suggests that transient cavity form is relatively invariant for impact craters and basins of all sizes (Melosh 1989), and therefore the concept is often useful (Croft 1981; Grieve 1991). The scaling between impact energy and transient cavity diameter is better understood than that between impact energy and main topographic rim diameter, because of the uncertainties in how the latter structure forms. Therefore, the transient cavity diameter may be more useful than the main ring diameter when describing the magnetic characteristics of an impact structure, especially if independent estimates of transient cavity diameters are available. For the purposes of our research, we use the results of Wieczorek and Phillips (1999) for transient cavity diameters (these authors use a crustal thickness model based upon LP gravity data to infer transient cavity diameters) where available (identified by WP in Table 1). Otherwise, we use the scaling relation of Croft (1985) (identified by C), which states that: $D_{tc} = D_r^{0.82} D_{sc}^{0.18}$ (where D_r is the main

ring diameter and D_{sc} is the simple-to-complex transition diameter, or ~18.7 km on the moon). This scaling relation may not be very accurate, and therefore, we check to ensure that we do not systematically underestimate or overestimate the transient cavity diameter for basins not investigated by Wieczorek and Phillips (1999). First, we consider the estimates of Wieczorek and Phillips as compared to those predicted by Croft's scaling relation for the same basins. The discrepancies are substantial, but there is no strong evidence of a systematic bias. For the ten basins considered, the ratio between the diameters predicted by Croft's scaling ratio to those determined by Wieczorek and Phillips ranges from 0.58 to 1.24, with a mean of 0.93 and a standard deviation of 0.23. As a further check, we can apply the results of recent studies of the terrestrial Chicxulub structure, which place the transient cavity diameter of this multi-ring basin between the peak ring and the main rim, slightly outside the innermost topographic boundary of the basin (Morgan et al. 1997). This is also consistent with the results of Wieczorek and Phillips (1999), who find that the transient cavity rim tends to lie close to the second innermost basin ring. We checked the diameters predicted by Croft's scaling law for all basins surveyed, and found that none failed these criteria. We, therefore, believe that the scaling law of Croft (1985) provides a reasonable estimate of transient cavity diameter.

We present magnetic field measurements for all post-Australe basins that show evidence of possible basin-associated magnetic signatures in Fig. 1, Fig. 2, and Fig. 3. We have found that basins older than Australe have no significant basin-associated magnetic signatures (in fact, only a few of the basins which lie in the same age range as Australe have magnetic signatures). This could be a result of subsequent crater impacts which destroyed any magnetic signatures or of superposition of subsequently emplaced magnetic material. Each panel of Figs. 1–3 shows surface crustal magnetic fields measured by the LP electron reflectometer. The LP magnetic field data set is binned at 1° resolution (~30 km at the equator) and boxcar smoothed over 3° by 3°, allowing nearly complete coverage of lunar crustal fields with good resolution. The smallest basin we investigate has a diameter of 300 km. We, therefore, have a minimum resolution of 10 data points across basins, and a minimum resolvable wavelength (after smoothing) of 30% of a basin diameter. Since the binning scheme is equal-angle (because of the polar orbit of LP, which ensures approximately equal-angle data coverage), resolution improves for basins farther from the equator. For all but the smallest equatorial basins, therefore, our resolution exceeds that estimated above. After binning and smoothing the magnetic field data, we average magnetic fields and plot versus distance from the basin center (normalized by basin main ring radius). The four traces in each panel (each averaged over 90° in angle) alternate between dashed and solid lines as shown in the bottom right of each figure (for example, trace number 1 is solid and shows

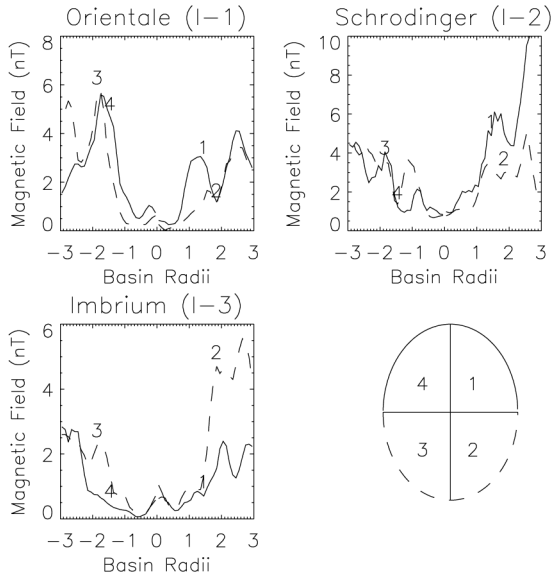

Fig. 1. Magnetic field profiles for three Imbrian basins, listed by name and age group. Fields are averaged over 90 degrees and plotted versus distance from the basin center (normalized by basin radius). The basin and surrounding areas are separated into numbered quadrants (northern quadrants shown by solid lines, southern by dashed) as shown by the circle at lower right.

average fields for the northeast quadrant of the basin and surrounding area). These plots show the radial dependence of the basin-associated magnetic fields, and also indicate their symmetry properties.

Fig. 1 shows magnetic field profiles for the three Imbrian basins. All three show clear symmetric demagnetization signatures centered over the basins (though extending well beyond the main basin rings). Orientale and Imbrium are two of the largest lunar basins, and data coverage over these basins is very good. We can, therefore, resolve their magnetic fields quite clearly, and can even identify very weak magnetic field enhancements in the basin centers.

Fig. 2 shows magnetic field profiles for eleven Nectarian basins. These magnetic signatures show a range of different types, including nearly complete demagnetization (Hertzsprung, Sikorsky-Rittenhouse), partial demagnetization (Serenitatis), demagnetization with magnetic anomalies in the center (Humorum, Mendeleev, Nectaris), and strong central magnetic anomalies (Bailly, Crisium, Humboldtianum, Mendel-Rydberg, Moscoviense).

Fig. 3 shows magnetic field profiles for 11 pre-Nectarian basins. These again show a range of magnetic signatures, ranging from clear demagnetization signatures (Grimaldi, Coulomb-Sarton, Poincare) to very strong central magnetic anomalies (Planck).

Most basins have magnetic signatures that are well-centered on the basins, as indicated by the close correspondence of the 4 magnetic field profiles near the basin centers. However, a few basins, such as Humboldtianum and

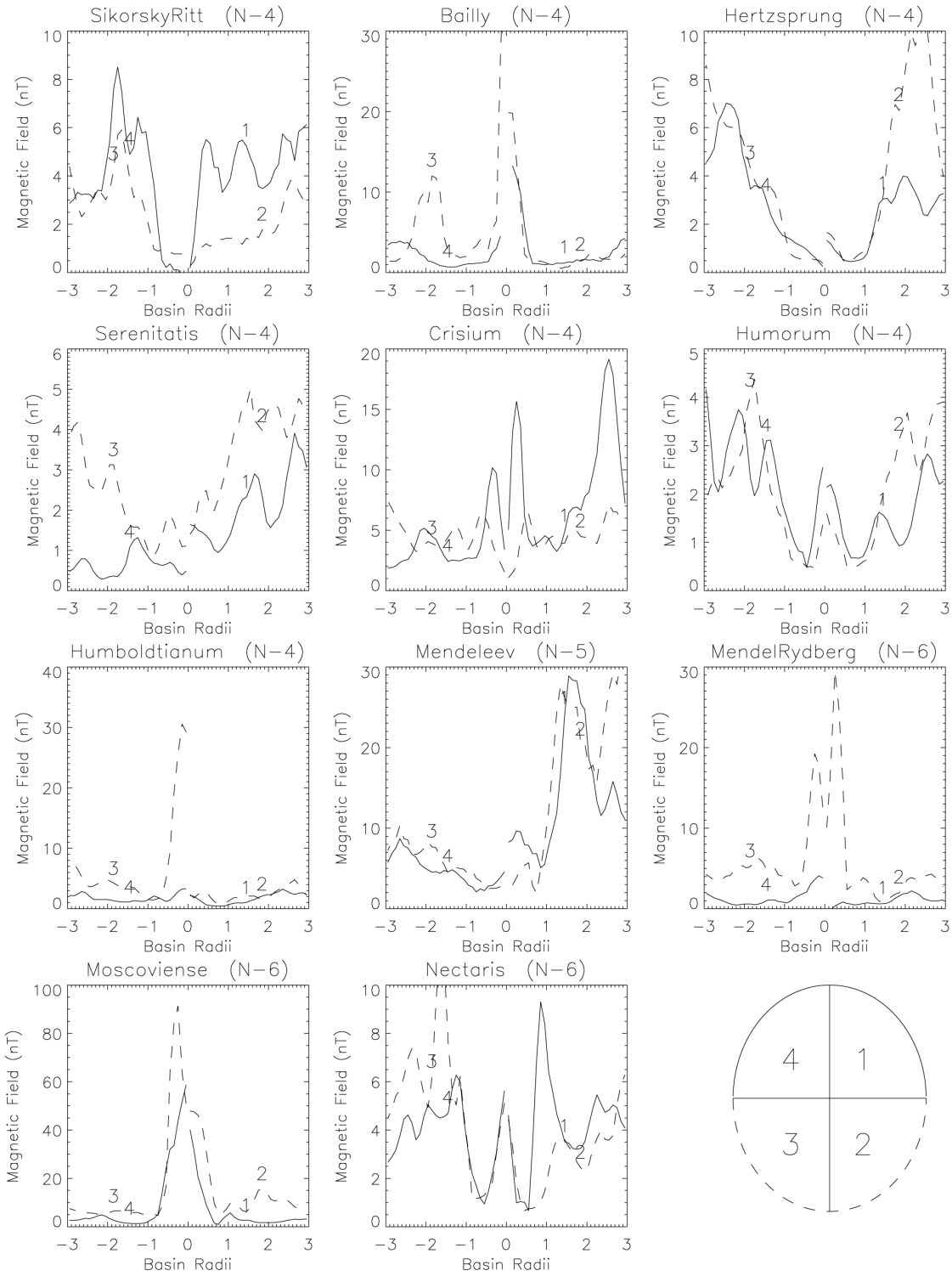

Fig. 2. Magnetic field profiles for eleven Nectarian basins, listed by name and age group. Fields are averaged over 90 degrees and plotted versus distance from the basin center (normalized by basin radius). The basin and surrounding areas are separated into numbered quadrants (northern quadrants shown by solid lines, southern by dashed) as shown by the circle at lower right.

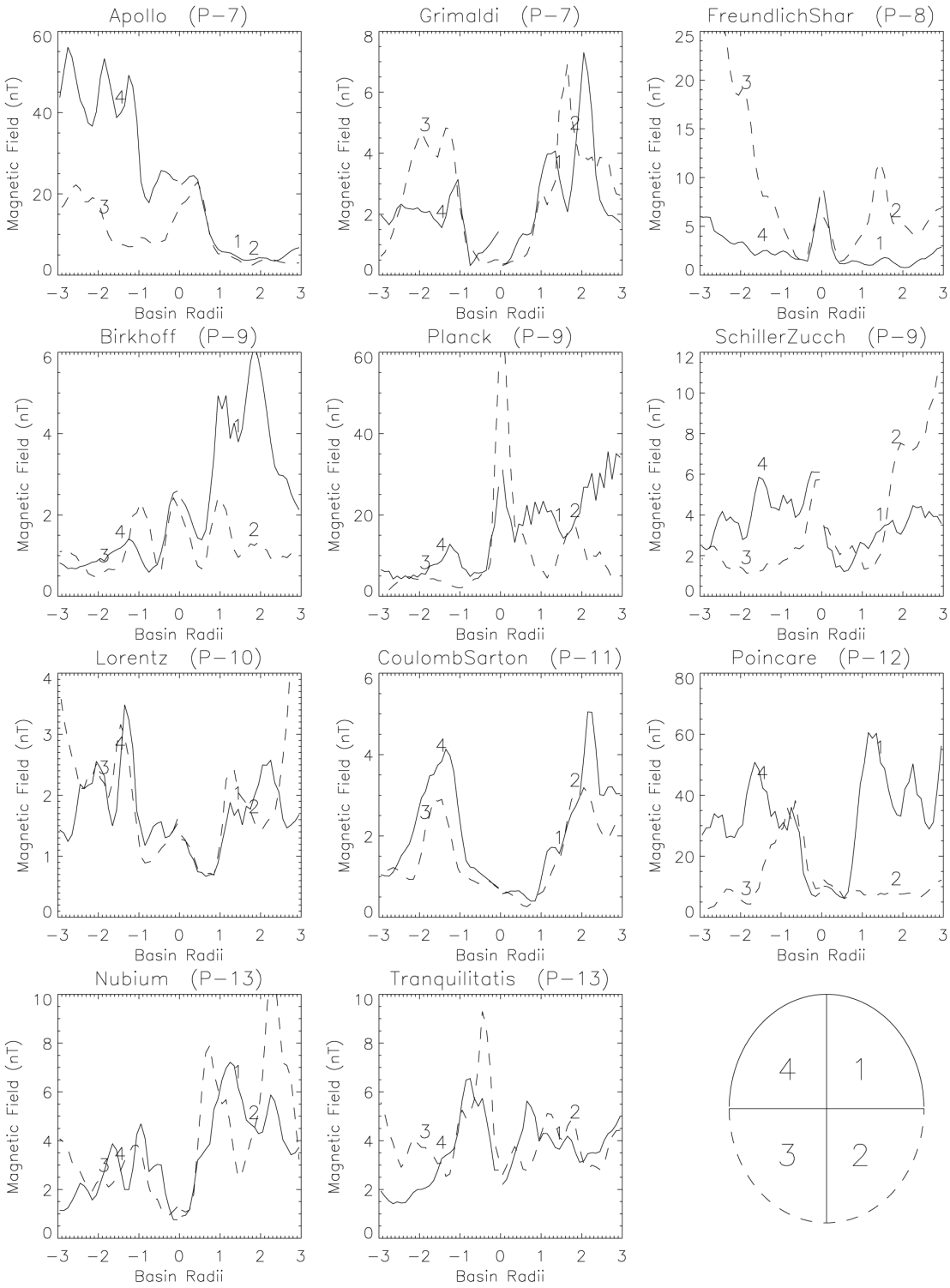

Fig. 3. Magnetic field profiles for eleven pre-Nectarian basins, listed by name and age group. Fields are averaged over 90 degrees and plotted versus distance from the basin center (normalized by basin radius). The basin and surrounding areas are separated into numbered quadrants (northern quadrants shown by solid lines, southern by dashed) as shown by the circle at lower right.

Mendel-Rydberg, have somewhat offset magnetic signatures. In both of these cases, magnetic anomalies fill most of the transient cavity region. However, the southern portions of these anomalies have much stronger fields than the northern.

The magnetic signatures of Mendeleev, Apollo, Freundlich-Sharonov, Planck, and Poincare are partially superimposed upon a strong regional magnetic field trend due to their location near the strongly magnetic antipodal regions. We do not show magnetic fields for the Korolev, Smythii, Ingenii, Keeler-Heaviside, and Lomonosov-Fleming basins, since we cannot identify any basin-associated magnetic signatures (presumably obscured by more recent magnetization) due to their location in the strongly magnetic antipodal regions. Two other old basins (Fecunditatis and Australe) lie in regions of weaker fields, but have no clear basin-associated magnetic signatures, and we do not show their magnetic fields.

We have considered the possibility that the apparent association of magnetic features with basins is due to random chance. We observe a variety of different magnetic signatures for lunar basins, and this may appear to lend support to this possibility. However, nearly all of the basin- associated magnetic signatures we observe are well correlated in location with the basins and can be roughly classified as magnetic anomalies that extend to ~0.5 basin radii, magnetic lows that extend to ~1–2 basin radii, or a superposition of these two basic types of signatures. If one picked a random spot and constructed magnetic field profiles, one might find a magnetic extremum, but it is quite unlikely that its width would correspond to anything physical. The fact that we can split the basin-associated magnetic signatures into two basic types (or a superposition of those two) with widths that correspond to a specific fraction of the radii of the basins in question provides strong evidence that the association of these magnetic features with the basins is real.

THE ORIENTALE AND IMBRIUM BASINS: OBSERVATIONS

Our best impact demagnetization data are for Orientale and Imbrium. These basins are large enough to ensure very good data coverage, and young enough that their magnetic signatures do not appear to have been significantly affected by more recent magnetization and demagnetization events. Fig. 4 shows profiles of magnetic field (averaged over all angles) versus distance from the basin centers (in units of basin radii [right side] and transient cavity radii [left side]) for Orientale and Imbrium. For both basins, the demagnetization process was quite efficient, with fields inside the basins reduced by a factor of 6–10. Observed magnetic lows extend well outside of the main basin rims. This agrees with the results of Scott et al. (1997), who found that the demagnetization of some terrestrial craters must extend outside of the main rim to account for observed magnetic signatures. However, in the lunar case, this effect is much more pronounced.

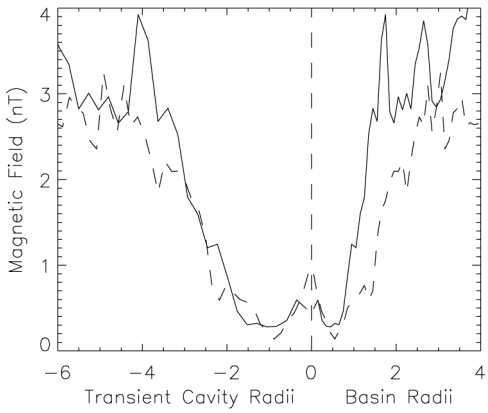

Fig. 4. Magnetic field (averaged over all angles) versus distance from the basin center (normalized by basin radius on the right, transient cavity radius on the left) for Orientale (solid line) and Imbrium (dashed).

The demagnetization of the Imbrium basin extends farther relative to its main topographic rim than that for Orientale. However, the more important fundamental quantity is probably the demagnetization extent relative to the transient cavity rim, since the relationship of the main topographic rim to the transient cavity rim depends on many factors (and the identification of the main rim is often ambiguous and fraught with difficulty). When normalized by transient cavity radii, the correspondence of the magnetic field profiles over Imbrium and Orientale becomes quite remarkable. Other than a peak at ~4 transient cavity radii from the center of Orientale (due to a strong magnetic anomaly at ~120°W, 20°S that lies antipodal to the Crisium basin), the magnetic profiles over Imbrium and Orientale are now virtually identical. Both basins show demagnetization effects extending to 3–3.5 transient cavity radii, with the most complete demagnetization lying inside of two transient cavity radii. There is a slight upturn in the magnetic field profiles near the basin centers (inside the transient cavity radii), possibly indicating some kind of remagnetization. It is possible that the close correspondence between the normalized magnetic profiles is fortuitous. However, we believe that this result indicates that both basins have been demagnetized by the same process. Shock pressure attenuation should scale approximately with transient cavity diameter, and normalizing by transient cavity diameter should produce closer correspondence in demagnetization signatures (as it does here) if shock demagnetization is indeed responsible.

BASIN MAGNETIC SIGNATURES VERSUS AGE: OBSERVATIONS

The evidence for slightly stronger magnetic fields in the central regions of the Orientale and Imbrium basins suggests

that, as for terrestrial basins, the primary magnetic lows over lunar basins may be modified by the presence of magnetic anomalies in the basin centers. We investigate magnetic profiles for older basins to see if this is a general trend. Fig. 5 shows average magnetic field profiles for all basins outside of the strongly magnetic antipodal regions (thus eliminating Korolev, Smythii, Keeler-Heaviside, Ingenii, and Lomonosov-Fleming). We remove basins with insufficient data coverage (Amundsen-Ganswindt and Mutus-Vlacq) from consideration. We separate the remaining basins into Imbrian, Nectarian, and pre-Nectarian age groups, and calculate magnetic field profiles for each group by averaging the magnetic field profiles (averaged over all angles, and normalized by transient cavity radii) of the individual basins in that group. These plots do not address the variability of the magnetic signatures of basins of the same age, which the individual panels of Fig. 1–3 show to be substantial. However, differences between the average magnetic profiles of different groups are not caused by only one or a few basins (with the exception of Planck, discussed further below), and we therefore consider them meaningful.

The observed basin magnetic signature changes radically as a function of age. For all basins, there is at least some evidence of a magnetic low around the basin (though this is not very significant for the pre-Nectarian basins). This low extends to 3–4 transient cavity radii for Imbrian and Nectarian basins. However, the suggestion of higher magnetic fields inside the transient cavity rim that we found for Imbrium and Orientale is greatly amplified for the Nectarian and pre- Nectarian basins. The central magnetic anomaly is, on average, the dominant observable signature for these older basins. These central anomalies, in general, extend approximately to the edge of the transient cavity. The average radial extent of the pre-Nectarian anomalies is less than that for the Nectarian anomalies, but this is largely a result of the very strong localized anomaly associated with the Planck basin, which dominates the average for the pre-Nectarian basins. The Planck magnetic anomaly is not very extensive, and data coverage over it is sparse, so any results that depend heavily upon Planck must be interpreted with some care. Without Planck included, the pre-Nectarian basins, on average, have much less significant central magnetic anomalies.

We separate Nectarian basins into age ranges N-4 to N-5 and N-6 in Fig. 6, and pre-Nectarian basins into age ranges P-7 to P-9 and P-10 to P-13 in Fig. 7. We find that the strongest central magnetic anomalies lie in the oldest Nectarian basins (average peak field of 21 nT), while younger Nectarian basins have more moderate anomalies (6 nT). Meanwhile, the younger pre-Nectarian basins also have strong anomalies (18 nT, though without the Planck basin included, the average peak central field is a more moderate 7 nT). The oldest pre-Nectarian basins have no apparent central anomalies.

We find that the common primary magnetic signature of

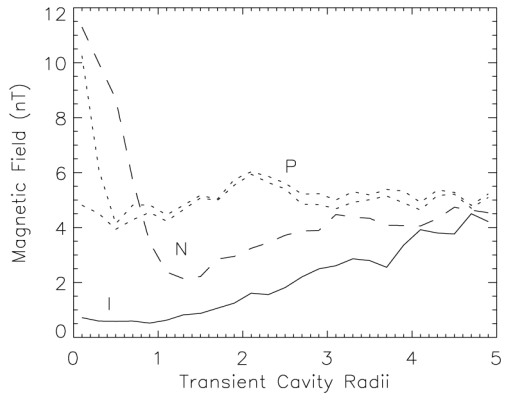

Fig. 5. Magnetic field (averaged over all angles) versus distance from basin center (normalized by transient cavity radius) for 3 Imbrian (solid line), 11 Nectarian (dashed line), and 13 pre-Nectarian basins (dotted lines, upper line with Planck included, lower line without).

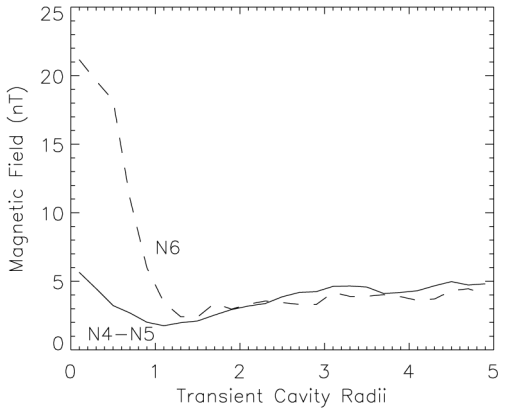

Fig. 6. Magnetic field (averaged over all angles) versus distance from basin center (normalized by transient cavity radius) for 8 basins in the N-4 to N-5 age groups (solid line) and 3 basins in the N-6 age group (dashed line).

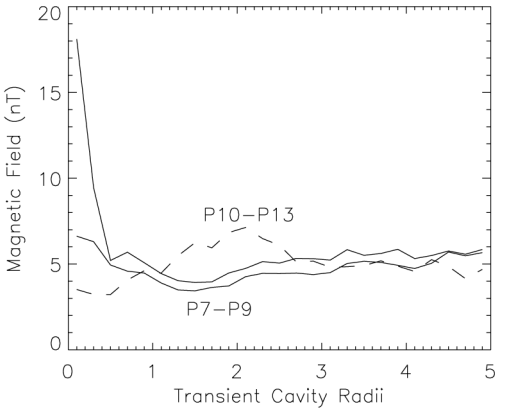

Fig. 7. Magnetic field (averaged over all angles) versus distance from basin center (normalized by transient cavity radius) for 6 basins in the P-7 to P-9 age groups (solid lines, upper line with Planck included, lower line without) and 7 basins in the P-10 to P-13 age groups (dashed line).

most lunar basins is a magnetic low. However, a secondary signature for many basins is the presence of a central magnetic anomaly. The observed central anomaly strength roughly follows an average age profile which is low (or nonexistent) for early pre-Nectarian basins, moderate for most late pre-Nectarian basins (though there is some evidence that the Planck basin has a rather strong central anomaly), high for early Nectarian basins, moderate for late Nectarian basins, and very low for Imbrian basins.

BASIN DEMAGNETIZATION: INTERPRETATION AND IMPLICATIONS

Recent research has demonstrated the primary importance of impact demagnetization in modifying the lunar crustal magnetic field distribution (Halekas et al. 2001, 2002a). We have found that impact craters and basins ranging in diameter from our effective resolution limit of ~50 km up to 1200 km (for the Imbrium basin) show clear evidence of demagnetization relative to their surroundings. Demagnetized craters and basins exist everywhere on the moon, in terranes with widely varying ages and magnetic fields. Reduced magnetic fields can extend to distances of ~2–4 crater or basin radii, providing clues to the nature of the demagnetization mechanism(s).

Modeling of the shock pressures generated by impacts was performed by Ahrens and O'Keefe (1977) using detailed equations-of-state and finite-difference schemes. They found that peak shock pressures along the impact symmetry axis (the vertical axis) are nearly constant in the near-field regime (though there is some slight attenuation), then decay rapidly in the far-field regime (beyond ~2–5 impactor radii). Far-field attenuation rates depend on impactor and target density, as well as impact velocity, but the peak shock pressures are generally well fit by a power law with a typical power of ~–2. This corresponds closely with reconstructed attenuation rates from terrestrial impact craters (Robertson and Grieve 1977) and with simpler models using a modified Murnaghan equation of state (Grieve and Cintala 1992). Another model for shock pressure decay was obtained by Melosh (1989), who used an empirical determination of particle velocity decay and the Hugoniot equation to derive:

$$P(r) = \rho_0[C + S(r_0/r)^{1.87}]u_0(r_0/r)^{1.87}$$

Here ρ_0 represents the un-shocked target density, C and S are empirically determined shock parameters, and u_0 is the initial particle velocity at distance r_0 from the impact point.

On-axis calculations cannot be directly used to determine the radial distribution of shock pressures near the surface. The attenuation rate is roughly the same, but peak shock pressures are lower near the surface due to interference between the impact-generated shock wave and rarefaction waves generated by interactions with the surface. Peak shock pressures scale roughly with the angle from the vertical axis as $\cos^{2\beta}\theta$, where β is the initial ratio of target to projectile compression (close to unity for similar projectile and target materials) and θ is the angle from the vertical axis (Grieve and Cintala 1992). The best way to determine the radial distribution of near-surface shock pressures is to use observations and modeling of shock zoning from terrestrial craters and basins, which imply peak shock pressures at the transient cavity rim of 1–2 GPa (Robertson and Grieve 1977; Kieffer and Simonds 1980).

For the purposes of this investigation, we adopt a simple peak shock pressure model which decays radially as r^{-2} in the far-field regime, and set the peak pressure at the transient cavity rim to 2 GPa. The data for Imbrium and Orientale (Fig. 4) show essentially complete demagnetization inside ~1.5–2 transient cavity radii. Our simple model predicts peak shock pressures of 0.5–0.9 GPa at these distances. We attempt to check this conclusion using the equation from Melosh (1989). Using the planar impact approximation (which states that peak shock pressure is relatively constant for $r_0 < r_p$ [the projectile radius]), Ahrens and O'Keefe (1977) estimated peak particle velocities of 3.75 and 7.5 km/s for a gabbroic anorthosite projectile impacting a gabbroic anorthosite target at 7.5 and 15 km/s respectively. We use $\rho_0 = 3965$ kg/m^3, C = 7.71 km/s and S = 1.05, appropriate for gabbroic anorthosite (Melosh 1989). We then apply the Schmidt-Housen (Schmidt and Housen 1987) scaling law to predict r_p for Imbrium. This gives Imbrium projectile radii of 104 km and 70 km for projectile velocities of 7.5 and 15 km/s. Plugging these back into the pressure equation gives peak shock pressures of ~2.5–5 GPa at distances of 1.5–2 transient cavity radii (regardless of whether we choose 7.5 or 15 km/s as the projectile velocity), which greatly exceed our previous estimates. In fact, we believe these pressures are unrealistically high, and that this formalism does not adequately take into account near-surface attenuation of shock waves. This equation would predict peak pressures of ~10 GPa at the transient cavity rim, rather than the 1–2 GPa suggested by terrestrial observations. When we set the pressure to 2 GPa at the transient cavity rim, the Melosh equation predicts pressures of 0.55–1.0 GPa at 1.5–2 transient cavity radii, almost the same as our simpler model. In the end, it appears that the predicted pressures mostly depend upon the assumed peak pressure at the transient cavity rim rather than the model chosen for attenuation rate. We prefer to rely on terrestrial observations, which suggest lower peak shock pressures. Even if we accept the higher estimates, however, these data show that crustal magnetization is almost completely removed by shock pressures of a few GPa, implying fairly soft average magnetization (the experimental work of Pohl et al. [1975] showed that a shock pressure of 1 GPa is roughly equivalent to AF demagnetization to 20 mT in its effect on terrestrial basalts).

Both thermal and shock effects can demagnetize magnetic carriers. However, in the case of lunar impacts, we

can easily determine that shock should be a much more important demagnetizing agent. Laboratory experiments show that shock pressures of a few tenths of a GPa to a few GPa can demagnetize terrestrial and lunar rocks (Cisowski et al. 1975; Cisowski and Fuller 1978; Pohl et al. 1975). On the other hand, temperatures of ~770°C are needed to thermally demagnetize Fe grains. Post-shock temperatures this high can only be generated by shock pressures of ~10 GPa in lunar fines (Ahrens and Cole 1974), and even higher shock pressures (on the order of 50 GPa) are needed to generate these post-shock temperatures in more competent rocks (Grieve et al. 1996). Therefore, it is clear that shock demagnetization should always be more important than thermal demagnetization on the moon. In fact, since terrestrial observations indicate peak pressures at the transient cavity radius of only ~2 GPa or less, thermal demagnetization effects should only be effective well inside this radius. The demagnetization signatures that we observe, extending to ~1.5–2 main rim radii, must therefore be due primarily to shock effects.

The absence of edge effects (see, e.g., Russell et al. [1977]) around demagnetized basins is also significant. If there was a magnetization contrast at the edge of a basin due to demagnetization of part of a region of homogeneous magnetization (or due to uniform magnetization in the basin itself), then one would observe a magnetic signature due to the magnetization contrast. If shock demagnetization is responsible, the demagnetization boundary is probably gradual rather than sharp, which will somewhat reduce the expected magnetic field signature. However, as a first approximation we can model the edge effect by treating a large basin such as Imbrium as a puncture in a uniformly magnetized sheet. We can estimate any edge effect for Imbrium as less than 1 nT in strength, which for typical parameters implies a magnetization contrast of $\sim 5 \times 10^{-7}$ A m^2/kg. This is somewhat below the range of magnetizations commonly observed in returned samples, which is 10^{-6}–10^{-4} A m^2/kg (Fuller 1974), and therefore, implies a lack of significant uniform magnetization in the region surrounding Imbrium or in the basin itself (and similarly for other demagnetized basins). Clearly, significant magnetization does exist outside of Imbrium and other demagnetized basins, since we observe many magnetic anomalies outside of the basins (though not inside). Therefore, the surrounding magnetization cannot be coherent, but instead must be jumbled in strength and/or polarity. Imbrium is so large that it can only provide a loose constraint on the background magnetic coherence scale, but a stronger one can be inferred from the demagnetization signatures of smaller craters, which suggest a coherence scale <25–50 km (Halekas et al. 2002a). The demagnetization signatures of smaller craters provide further evidence that there is no significant uniform magnetization in the demagnetized basins themselves, since we do not observe edge effects around younger craters in these basins.

CENTRAL MAGNETIC ANOMALIES: INTERPRETATION AND IMPLICATIONS

Many lunar basins have central magnetic anomalies similar in radial extent to the outer anomalies of the Chicxulub basin (which have been interpreted as magnetized impact melt) (Pilkington and Hildebrand 1994), and therefore, by analogy, the lunar anomalies may also be at least partially due to TRM in the basin melt sheets. The fact that the anomalies extend roughly to the edge of the transient cavity may provide evidence for this scenario, as the most substantial volumes of basin impact melt lie within the transient cavity region (especially in large basins) (Spudis 1993; Cintala and Grieve 1998). However, SRM in uplifted material could also be partially or fully responsible for the observed magnetic fields. The diameter of the structural uplift of impact basins has been estimated as $D_{su} = 0.31 D_r^{1.02}$ (Therriault et al. 1997), or ~50–60% of the transient cavity diameter. Though many magnetic anomalies ascribed to SRM in uplifted material in terrestrial basins do not extend this far radially (Pohl et al. 1988; Coles and Clark 1978, 1982), uplift-associated anomalies certainly could extend to the edges of the central uplift region. This would remain smaller than the observed extent of most lunar central basin magnetic anomalies, but not by a large factor. The basin-associated magnetic fields tend to peak in the center of the basins (Crisium is a notable exception) which could imply higher thicknesses of melt (if the anomalies are due to TRM) or higher magnetization due to higher pressures (if SRM). We must also remember that remanence carriers on the moon differ from those on the Earth, with lunar remanence primarily carried by metallic iron rather than iron oxides (Fuller 1974). Since reduction due to impact-generated shock appears to be an important process for producing these metallic iron remanence carriers (Fuller and Cisowski 1987), impacts may produce more remanence carriers in the center of basins. These sources could then be magnetized by either TRM or SRM.

A fundamental question is: does the existence of the central basin magnetic anomalies imply the presence of an active lunar core dynamo at the time of basin formation? Unfortunately, we find it difficult to answer this question. We can only compare to terrestrial basins, which were, of course, created in the presence of a dynamo field. However, did the production of the basin-associated anomalies required the presence of the dynamo field? In cases where researchers have measured or inferred the remanent magnetization directions in terrestrial basins, it appears that the magnetic carriers were magnetized by the dynamo field. However, could another magnetizing field have filled this role equally well in the lunar case? A measurement of the polarity of the lunar central basin anomalies would help answer this key question. Unfortunately, reflectometer data can only provide the field magnitude. Magnetometer data could determine

polarity, but it is unfortunately likely that a magnetometer at orbital altitude could not detect most of these anomalies.

We find that the average magnetic signature of lunar impact basins changes with age. The central basin magnetic anomalies, on average, vary in peak magnetic field, with weaker fields in Imbrian and pre-Nectarian basins, and the strongest fields in early Nectarian basins (though we also find evidence for a strong anomaly in the late pre-Nectarian basin Planck). It is difficult to know how much stock to put in these observations, since we are out of necessity working with a very limited sample of basins, and subsequent magnetization and demagnetization events may affect the magnetic signatures of older basins. However, the differences as a function of age may still be significant. All three Imbrian basins have very weak central basin fields. Of the Nectarian basins, five have strong central anomalies (tens of nT), four more have moderate anomalies of a few nT, and only two (Serenitatis and Sikorsky-Rittenhouse) have no clear anomalies. Of the pre-Nectarian basins, only Planck has a strong anomaly, five more basins have moderate anomalies, and five have no clear anomaly. We cannot, therefore, explain the observed differences in magnetic signatures as due to just a few basins.

If one accepts the differences in the magnetic properties of basins of different ages, the clear question is: does this have anything to do with the lunar magnetic environment when the basins formed? It is a fact that both TRM and SRM produce remanent magnetization whose strength depends on the magnitude of the ambient magnetic field (Fuller and Cisowski 1987). However, the strength of magnetization produced could also depend on other elements, including impact size, impactor or target characteristics, or other properties of the ambient magnetic field. It seems unlikely that any of these should vary systematically with age. However, a bias in our sample also remains a possibility. We cannot determine the presence of biases in many of the above factors, but we did investigate several candidates, including basin transient cavity diameter (a proxy for impact energy) and basin location (a proxy for target characteristics). We found no clear biases in either of these parameters, other than the fact that Imbrian basins are larger on average (because of Imbrium and Orientale). As another way of attacking this question, though, we attempted to find a dependence of magnetic field characteristics on these parameters, regardless of basin age. We first split up basins into groups with different ranges of transient cavity diameters. We did find a tendency for the smallest size groups to have the strongest average central anomaly signatures. However, we found that this dependence was almost entirely due to the three basins with the strongest central anomalies, namely Bailly, Planck, and Moscoviense. It is intriguing that all three of these strongly magnetized basins are rather small. However, when we remove these three basins, all trace of a size dependence vanishes. Any size dependence, then, is much less robust than the observed age dependence. We followed a similar procedure in splitting up basins into groups according to location on the lunar surface and found no evidence of a location dependence. Clearly, none of this analysis proves anything. Due to the small sample sizes, we cannot make any unequivocal conclusions. Obviously, more than one possible explanation exists for the observed variation in the magnetic characteristics of basins of different ages. However, the presence of lunar crustal magnetic anomalies (assuming that their creation required some kind of ambient magnetic field), along with the current absence of strong ambient fields, suggest an ambient lunar magnetic field that has changed over time. Furthermore, we see no clear reason to expect most other parameters to vary systematically with basin age. Perhaps the simplest hypothesis, therefore, is that the variation in basin anomaly strength at least partially reflects the magnetic field history of the moon. We intend to explore the implications of this hypothesis. We do not know how factors other than magnetizing field may have affected the basin anomalies (or indeed, what these factors may be). However, other processes entirely could certainly have produced the observed age dependence, and therefore our conclusions can only be tentative.

If TRM in melt rocks produced the basin anomalies, this implies the presence of a strong and steady ambient magnetic field while the impact melt sheet cooled (the time for a 2.5 km thick melt sheet to cool below the Fe Curie point can be estimated as ~0.5 million years, with cooling times for thicker melt sheets scaling roughly as $[\text{thickness}]^2$ (Ivanov et al. [1997]). A natural candidate to produce such a field is a lunar core dynamo. This also provides the simplest explanation for the remanent magnetization found in returned lunar samples. It is suggestive that, if basin anomalies do in fact reflect the strength of the magnetizing field, both the basin anomalies and the samples provide evidence for a "magnetic era" of sorts. However, while paleointensity results imply strong fields in Nectarian and early Imbrian times (~3.6–3.9 Ga) (Fuller and Cisowski 1987), central basin anomalies suggest peak fields in early Nectarian times and weaker fields in Imbrian times. Unless there were much stronger paleofields in Nectarian times than those implied by the samples so far measured, we find a discrepancy in the timing of the peak magnetic fields. This disagreement only amounts to ~250 million years at the most (not a long time, geologically speaking). However, unless basin-associated magnetization was not emplaced until a few hundred million years after the formation of the basins, the discrepancy still exists. The long cooling times for thick impact melt sheets could explain delays of a few million years, but almost certainly not hundreds of millions of years.

One expects to observe some differences in the magnetic field histories implied by returned samples and basin-associated fields, since the cumulative effects of impact demagnetization should have different effects upon the

samples (collected on the surface) and the basin anomalies (presumably deep-seated), especially if their magnetic characteristics differ. However, it is not clear that this effect can lead to a discrepancy as great as the one we observe. One could also suggest that if the ambient field was due to a dynamo that reversed on a time scale short compared to the cooling time of an impact melt sheet, coherent remanent magnetization would not be produced, even in the presence of a strong field. However, postulating the existence of a dynamo with a reversal rate, which is slow in Nectarian and pre-Nectarian times but rapid in Imbrian times, seems a rather desperate contrivance. One could also suppose that younger basins have magnetization as strong as that in older basins, but that it is uniform, and therefore, produces no significant magnetic fields. However, we should still see significant fields at the edges of a uniformly magnetized sheet or around any punctures in it. Therefore, the absence of edge effects around Imbrian basins and around younger superposed craters strongly argues against this possibility.

If Nectarian and pre-Nectarian basins formed in the presence of a strong and steady ambient field, we might find the lack of evidence of strong TRM for contemporaneous geologic terranes somewhat surprising. The strongly magnetic antipodal regions were likely magnetized by SRM rather than TRM. Outside of the antipodal regions, many localized strong magnetic anomalies exist, but no widespread surficial terranes have average magnetic fields stronger than ~5 nT, thus constraining the strength of any TRM. However, central basin melt sheets could be thicker than other coherently magnetized lunar terranes, and would, therefore, produce the strongest magnetic fields and remain least vulnerable to impact demagnetization. By analogy with the Sudbury basin on Earth, which has a melt sheet 2–5 km thick in a basin 200 km in diameter (Grieve 1991), we may expect the largest lunar basins to have melt sheets of up to 12–30 km in thickness. Calculations taking into account the relative melting efficiency on the moon suggest a melt sheet thickness of >3.5 km for the Schrodinger basin (320 km in diameter), which would similarly imply melt thicknesses of ~14 km (or even more, since the relative melting efficiency increases with diameter) for the largest lunar basins (Cintala and Grieve 1998). Therefore basin melt sheets, even for the smaller basins, could easily be the thickest coherently magnetized lunar terranes.

If TRM in impact melt did not produce the observed magnetic anomalies, SRM in the unmelted materials raised near the surface in the central uplift may instead be responsible, though it seems less likely that this magnetization would extend as far radially as the observed anomalies. It remains unclear how deep the shock pressures necessary to generate strong and stable magnetic remanence extend, especially since uplift compresses strata. However, measurements below the terrestrial Puchezh-Katunki impact basin (80 km diameter) implied peak shock pressures of ~40 GPa at the top of the central uplift and ~10 GPa five km below this (Ivanov 1994). These pressures could easily produce stable shock remanence (Cisowski and Fuller 1978; Pohl et al. 1975) but would not heat competent rocks above the Fe Curie point or melt them (Grieve et al. 1996), suggesting that shock could magnetize uplifted material to considerable depth in lunar basins.

If the central anomalies formed by SRM rather than TRM, it would eliminate the requirement that the ambient magnetic field remain steady over a long period of time. Unlike TRM, which requires long cooling times, SRM can take place on a very short time scale. Generation of SRM still requires the presence of a strong ambient field, but it could conceivably be created by impact-generated transient magnetic field amplifications like those possibly responsible for the antipodal anomalies (Hood and Huang 1991). However, model calculations predict that transient field amplifications produced by expansion of plasma from large impacts should peak at the antipode and remain weak at the impact point, thus suggesting that strong basin-associated SRM could be more easily generated in a dynamo field. Also, if the central anomalies were generated by SRM in transiently amplified fields, one would still expect to see strong magnetic anomalies associated with Imbrian basins as well as older basins. The fact that we only see strong anomalies over older basins still appears to imply that something about the lunar magnetic environment (or some other factor entirely) must have been different in Nectarian and pre-Nectarian times.

CONCLUSIONS

We observe two basic types of magnetic signatures for lunar impact basins. The primary signature, present for basins of all ages, is a magnetic low extending to ~1.5–2 basin radii (~3–4 transient cavity radii). A secondary signature of many lunar basins is a central magnetic anomaly extending approximately to the edge of the transient cavity. These central anomalies, on average, describe a magnetic field age profile that peaks in early Nectarian times, possibly providing evidence of a similar variation in the magnetizing field.

The radial extent of basin-associated demagnetization signatures provides strong evidence that shock effects are responsible, since demagnetization effects extend outside of regions that should have seen significant heating. Comparison of magnetic data from demagnetized basins with modeled shock pressures implies a rather soft average lunar crustal magnetization (demagnetized by shock pressures of a few GPa). The relatively smooth demagnetization signatures (i.e., no edge effects) also show the lack of large scale coherence of the crustal magnetization. The relatively low coercivity and low coherence scale of lunar crustal magnetization may imply that transient shock-related processes were responsible for much of its formation.

The central basin magnetic anomalies may be due to

TRM in the impact melt sheets and/or in melt-rich breccias, or they could also be at least partially due to SRM in the central uplift region. The comparatively strong central magnetic fields in some basins may show that their magnetization has not been affected as severely as that of other lunar terranes by subsequent impact demagnetization, thus suggesting that basin magnetization may extend to substantial depths. This could argue for either TRM in the basin melt sheets or SRM in the central uplift. The fact that most anomalies extend approximately to the edge of the transient cavity may provide evidence that TRM in the basin melt sheets is the more likely explanation of the two. However, SRM in the central uplift or a combination of the two effects remain possible.

Whatever magnetization mechanism is responsible, if basin anomalies do provide a good measure of the magnetizing field, then the average age profile observed for the central anomaly strength suggests a "magnetic era" similar to that implied by paleointensity results from returned samples. Both of these results can be most easily explained by the presence of a lunar core dynamo. However, the basin anomalies imply low paleofields in Imbrian times and higher fields in early Nectarian times, while paleointensity results provide evidence for high fields in Nectarian and early Imbrian times (~3.6–3.9 Ga). It seems unlikely that all the paleointensity results for Imbrian-aged samples are wrong, especially since we observe strong crustal fields antipodal to Orientale and Imbrium (the antipodal magnetization most likely formed when the basins formed, and therefore, also suggests the presence of strong fields in Imbrian times, though these fields could have been transient in nature) (Lin et al. 1988). However, the observational evidence for a lack of strong crustal magnetization in Imbrian basins is also very strong. The cumulative effects of subsequent impact demagnetization (which will affect magnetization of varying depth and magnetic characteristics differently) upon both the returned samples and the basins may partly explain any discrepancy, but it is not at all clear that this effect can completely explain the observations. One could suggest that any differences result from the statistics of small numbers. However, statistics aside, the individual observation that Imbrium has no strong central magnetic anomaly, while older basins do, remains difficult to reconcile with sample data.

We could resolve this dilemma if we could show that basin anomalies do not provide a good measure of the ambient magnetic fields present when the basins formed. The magnetization process responsible for creating the central basin anomalies could produce magnetization with a strength that depends on variables other than the ambient magnetic field strength. These could include quantities such as impact scale, impactor and target characteristics, or other properties of the ambient magnetic field such as polarity, scale size, reversal rate (if due to a dynamo), etc. The magnetic fields that we observe also may not accurately reflect the strength of the crustal magnetization in the basins. Magnetic fields are observed over discontinuities or gradients in magnetization, and differences in the magnetic coherence scale and magnetization depth can lead to significant differences in surface magnetic fields. It is unclear what would cause a systematic variation with age for any of the quantities mentioned above or why it would produce a magnetic field age profile like the one we observe. It seems most likely that a combination of one or more of these effects and the results of impact demagnetization must cause the observed discrepancy in implied lunar magnetic histories, though. In the end, however, we still do not know enough about the intrinsic magnetic effects of basin-forming impacts to make any strong conclusions.

Acknowledgments–This work was partially supported by a NASA GSRP fellowship received by JSH. Some support was also provided by NASA through subcontract LRI-99-101 from the Lunar Research Institute and through grant NAG5-9305. We thank Lon Hood and Gareth Collins for thorough and helpful reviews which greatly improved this paper.

Editorial Handling—Dr. Elizabetta Pierazzo

REFERENCES

Ahrens T. J. and Cole D. M. 1974. Shock compression and adiabatic release of lunar fines from Apollo 17. Proceedings, 5th Lunar and Planetary Science Conference. pp. 2333–2345.

Ahrens T. J. and O'Keefe J. D. 1977. Equations of state and impact-induced shock-wave interaction on the moon. In *Impact and explosion cratering,* edited by Roddy D. J., Pepin R. O., and Merrill R. B. New York: Pergamon. pp. 639–656.

Anderson K. A., Lin R. P., McCoy J. E., and McGuire R. E. 1976. Measurements of lunar and planetary magnetic fields by reflection of low energy electrons. *Space Science Instrumentation* 1:439.

Cintala M. J. and Grieve R. A. F. 1998. Scaling impact melting and crater dimensions: Implications for the lunar crater record. *Meteoritics & Planetary Science* 33:889–912.

Cisowski S. M. and Fuller M. 1978. The effect of shock on the magnetism of terrestrial rocks. *Journal of Geophysical Research* 83:3441–3458.

Cisowski S. M., Fuller M. D., Wu Y. M., Rose M. F., and Wasilewski P. J. 1975. Magnetic effects of shock and their implications for magnetism of lunar samples. Proceedings, 6th Lunar and Planetary Science Conference. pp. 3123–3141.

Coleman P. J., Lichtenstein B. R., Russell C. T., Sharp L. R. and Schubert G. 1972. Magnetic fields near the moon. *Geochimica et Cosmochimica Acta* 36:2271–2286.

Coles R. L. and Clark J. F. 1978. The central magnetic anomaly, Manicougan structure, Quebec. *Journal of Geophysical Research* 83:2805–2808.

Coles R. L. and Clark J. F. 1982. Lake St. Martin impact structure, Manitoba, Canada: Magnetic anomalies and magnetizations. *Journal of Geophysical Research* 87:7087–7095.

Croft S. K. 1981. The excavation stage of basin formation: A qualitative model. In *Multi-ring basins,* edited by Schultz P. H. and Merrill R. B. New York: Pergamon Press. pp. 207–225.

Croft S. K. 1985. The scaling of complex craters. *Journal of Geophysical Research* 90:C828–C842.

Fuller M. 1974. Lunar magnetism. *Reviews of Geophysics and Space Physics* 12:23-70.

Fuller M. and Cisowski S. M. 1987. Lunar paleomagnetism. In *Geomagnetism,* edited by Jacobs J. Orlando: Academic Press. pp. 307–455.

Grieve R. A. F. 1991. Terrestrial impact: The record in the rocks. *Meteoritics* 26:175–194.

Grieve R. A. F. and Cintala M. J. 1992. An analysis of differential impact melt-crater scaling and implications for the terrestrial impact record. *Meteoritics* 27:526–538.

Grieve R. A. F., Langenhorst F., and Stöffler D. 1996. Shock metamorphism of quartz in nature and experiment: II. Significance in geoscience. *Meteoritics & Planetary Science* 31: 6–35.

Halekas J. S., Mitchell D. L., Lin R. P., Frey S., Hood L. L., Acuña M. H., and Binder A. B. 2001. Mapping of crustal magnetic anomalies on the lunar near side by the Lunar Prospector electron reflectometer. *Journal of Geophysical Research* 106:27841–27852.

Halekas J. S., Mitchell D. L., Lin R. P., Hood L. L., Acuña M. H., and Binder A. B. 2002a. Demagnetization signatures of lunar impact craters. *Geophysical Research Letters* 29(13).

Halekas J. S., Mitchell D. L., Lin R. P., Hood L. L., Acuña M. H., and Binder A. B. 2002b. Evidence for negative charging of the lunar surface in shadow. *Geophysical Research Letters* 29(10).

Hood L. and Huang Z. 1991. Formation of magnetic anomalies antipodal to lunar impact basins: Two-dimensional model calculations. *Journal of Geophysical Research* 96:9837–9846.

Hood L. L., Zakharian A., Halekas J., Mitchell D. L., Lin R. P., Acuña M. H., and Binder A. B. 2001. Initial mapping and interpretation of lunar crustal magnetic anomalies using Lunar Prospector magnetometer data. *Journal of Geophysical Research* 106: 27825–27840.

Ivanov B. A. 1994. Geochemical models of impact cratering: Puchezh-Katunki structure. *Geological Society of America Special Papers* 293:81–91.

Ivanov B.A., Deutsch A., Ostermann M., and Ariskin A. 1997. Solidification of the Sudbury impact melt body and nature of the offset dikes—Thermal modeling. Proceedings, 28th Lunar and Planetary Science Conference. pp. 633–634.

Kieffer S. W. and Simonds C. H. 1980. The role of volatiles and lithology in the impact cratering process. *Reviews of Geophysics and Space Physics* 18:143–181.

Lin R. P., Anderson K. A. and Hood L. 1988. Lunar surface magnetic field concentrations antipodal to young large impact basins. *Icarus* 74:529–541.

Melosh H. J. 1989. *Impact cratering: A geologic process.* New York: Oxford University. 245 p.

Melosh H. J. and Ivanov B. A. 1999. Impact crater collapse. *Annual Review of Earth and Planetary Sciences* 27:385–415.

Morgan J.V. et al. 1997. Size and morphology of the Chixculub impact crater. *Nature* 390:472–476.

Pike R. J. 1980. Control of crater morphology by gravity and target type—Mars, Earth, Moon. Proceedings, 11th Lunar and Planetary Science Conference. pp. 2159–2189.

Pilkington M. and Grieve R. A. F. 1992. The geophysical signatures of terrestrial impact craters. *Reviews of Geophysics* 30:161–181.

Pilkington M. and Hildebrand A. R. 1994. Gravity and magnetic field modeling and structure of the Chicxulub crater, Mexico. *Journal of Geophysical Research* 99:13,147–13,162.

Plado J., Pesonen L. J., Koeberl C., and Elo S. 2000. The Bosumtwi meteorite impact structure, Ghana: A magnetic model. *Meteoritics & Planetary Science* 35:723–732.

Pohl J., Bleil U., and Hornemann U. 1975. Shock magnetization and demagnetization of basalt by transient stress up to 10 kbar. *Journal of Geophysics* 41:23–41.

Pohl J., Eckstaller A., and Robertson P. B. 1988. Gravity and magnetic investigations in the Haughton impact structure, Devon Island, Canada. *Meteoritics* 23:235–238.

Robertson P. B. and Grieve R. A. F. 1977. Shock attenuation at terrestrial impact structures. In *Impact and explosion cratering,* edited by Roddy D. J., Pepin R. O., and Merrill R. B. New York: Pergamon. pp. 639–656.

Russell C. T., Coleman P. J., and Schubert G. 1977. On deducing the magnetization of the lunar surface from orbital surveys. *Physics of the Earth and Planetary Interiors* 13:386–390.

Schmidt R. M. and Housen K. R. 1987. Some recent advances in the scaling of impact and explosion cratering. *International Journal of Impact Engineering* 5:543–560.

Scott R. G., Pilkington M., and Tanczyk E. I. 1997. Magnetic investigations of the West Hawk, Deep Bay, and Clearwater impact structures, Canada. *Meteoritics & Planetary Science* 32: 293–308.

Spudis P. D. 1993. The geology of multi-ring impact basins: The moon and other planets. Cambridge: Cambridge University Press. 263 p.

Therriault A. M., Grieve R. A. F., and Reimold W. U. 1997. Original size of the Vredefort structure: Implications for the geological evolution of the Witwatersrand basin. *Meteoritics & Planetary Science* 32:71–77.

Wieczorek M. A. and Phillips R. J. 1999. Lunar multiring basins and the cratering process. *Icarus* 139:246–259.

Wilhelms D. E. 1984. Moon. In *The geology of the terrestrial planets,* edited by Carr M. H. Washington D.C.: NASA Science and Technology Information Branch. pp. 107–205.